

# Spin-phonon coupled modes in the incommensurate phases of doped $\text{CuGeO}_3$

K. Takehana, T. Takamasu, M. Hase, and G. Kido

*Nanomaterials Laboratory, National Institute for Materials Science, 3-13 Sakura, Tsukuba, Ibaraki 305-0003, Japan*

T. Masuda and K. Uchinokura

*Department of Advanced Materials Science, The University of Tokyo, 6th Engineering Building, 7-3-1 Hongo, Bunkyo-ku, Tokyo 113-8656, Japan*

(Received 22 September 2000; revised manuscript received 7 February 2001; published 5 June 2001)

The doping effect of the folded phonon mode at  $98 \text{ cm}^{-1}$  was investigated on Si-doped  $\text{CuGeO}_3$  by magneto-optical measurements in the far-infrared region under a high magnetic field. The folded phonon mode at  $98 \text{ cm}^{-1}$  appears not only in the dimerized phase but also in the dimerized-antiferromagnetic phase on the doped  $\text{CuGeO}_3$ . The splitting was observed in the incommensurate (IC) phase and the antiferromagnetically ordered incommensurate (IAF) phase above  $H_C$ . The split-off branches exhibit a different field dependence from that of the pure  $\text{CuGeO}_3$  in the vicinity of  $H_C$ , and the discrepancy in the IAF phase is larger than that in the IC phase. This is caused by the interaction between the solitons and the impurities.

DOI: 10.1103/PhysRevB.63.245413

PACS number(s): 78.66.-w, 78.30.-j, 63.22.+m

## I. INTRODUCTION

An inorganic compound  $\text{CuGeO}_3$  was discovered to undergo a spin-Peierls (SP) transition at a critical temperature  $T_{SP} = 14 \text{ K}$  in magnetic susceptibility measurements.<sup>1</sup> In the SP transition, the formation of a superlattice occurs owing to the coupling between a one-dimensional spin system and three-dimensional phonon systems, together with the opening of a magnetic energy gap between the singlet ground state and a triplet-excited state. The lattice dimerization was confirmed by electron diffraction,<sup>2</sup> x-ray diffraction, and neutron diffraction.<sup>3,4</sup> The opening of a spin gap due to the SP transition was directly observed by inelastic neutron scattering experiments.<sup>5</sup> A phase transition from a dimerized ( $D$ ) phase to an incommensurate (IC) phase was found at the critical field  $H_C \approx 12 \text{ T}$ .<sup>6</sup> The incommensurate lattice modulation was observed in x-ray measurements under a high magnetic field above  $H_C$ .<sup>7</sup> Higher-order harmonics of the incommensurate Bragg reflections were also observed just above  $H_C$ , which indicates that lattice modulation in the IC phase forms a soliton lattice.<sup>8</sup>

One of the most important studies enabled by the discovery of  $\text{CuGeO}_3$  is that of impurity effects on a quasi-one-dimensional spin system. For small amounts of an impurity, another phase transition to the dimerized-antiferromagnetic (DAF) phase was found at  $T_N$ , which is lower than  $T_{SP}$ .<sup>9</sup> In the DAF phase, the coexistence of the lattice distortion and the antiferromagnetic ordering was found in neutron-diffraction experiments.<sup>10-12</sup> Recently, Masuda *et al.* found a first-order compositional phase transition between the DAF and the uniform-antiferromagnetic phases in Mg-doped  $\text{CuGeO}_3$ .<sup>13</sup> It is not clear whether this kind of phase transition exists in Si-doped  $\text{CuGeO}_3$  or not, but the sample with low concentration used in this paper apparently has the nature of a DAF phase below  $T_N$ .<sup>14</sup> There are some reports about the nature of a high-field phase in doped  $\text{CuGeO}_3$  with a low concentration of impurities. Two phase transitions have been reported in specific heat experiments: one was the phase transition between uniform ( $U$ ) and IC phases, and the

other was a transition between the IC phase and the antiferromagnetically ordered incommensurate (IAF) phase.<sup>15</sup> On the other hand, ultrasonic velocity measurements have suggested only one phase transition occurred above  $H_C$ .<sup>16</sup> Recently, a different behavior between the IC and IAF phases was reported on the thermal conductivity.<sup>17</sup> The authors suggested that this is caused by a ‘‘freezing’’ of the solitons in the IAF phase.

Optical studies are quite sensitive for an investigation of the change in crystal structure that is caused by a phase transition. Factor group analysis predicts that nine infrared-active folded modes and 18 Raman-active folded modes appear below  $T_{SP}$  in addition to optical phonons in the  $U$  phase, which occur when the symmetry of the crystal structure is lowered from  $Pbmm$  of the  $U$  phase<sup>18</sup> to  $Bbcm$  of the  $D$  phase.<sup>4,19</sup> Three Raman modes at 107, 369, and  $820 \text{ cm}^{-1}$  were assigned to the  $A_g$  folded phonons in the  $D$  phase,<sup>20</sup> with the first one having a Fano-type line shape.<sup>21,22</sup> For infrared-active folded phonons, one  $B_{3u}$  mode, one  $B_{1u}$  mode, and two  $B_{2u}$  modes were found at 98, 284, 312, and  $800 \text{ cm}^{-1}$ , respectively.<sup>23-25</sup> The field dependence of the folded-phonon modes was investigated in Raman experiments.<sup>26,27</sup> The intensity decreases steeply at the boundary between the  $D$  and IC phases, while no energy shift is observed. Just above  $H_C$ , the intensity decreases to about half that of the  $D$  phase, and continues to decrease in the IC phase with increasing field. The folded mode at  $312 \text{ cm}^{-1}$  was observed above  $H_C$ , but the details were unclear because it is located on the shoulder of an optical phonon.<sup>28</sup>

In contrast to these results, in our previous paper<sup>25</sup> we found a splitting of the folded-phonon mode at  $98 \text{ cm}^{-1}$  in the IC phase. The energy separation between the split-off branches is proportional to the incommensurability in the IC phase. This indicates that the incommensurability is closely related to the mechanism of splitting of a folded phonon in the IC phase. In the IC phase, the phonon modes at  $\mathbf{k} = \pm(\mathbf{q}_{SP} - \Delta\mathbf{q})$  can be infrared active due to the incommensurate lattice modulation.<sup>29</sup> We have explained this phenom-

enon as follows: the  $98\text{-cm}^{-1}$  phonon is a spin-phonon coupled mode. Because of this the phonon mode at  $\mathbf{k}=\mathbf{q}_{SP}-\Delta\mathbf{q}$  and that at  $\mathbf{k}=-(\mathbf{q}_{SP}-\Delta\mathbf{q})$  can interact with each other through the spin component  $2\Delta\mathbf{q}$  of a static incommensurate spin and lattice structure in the IC phase. The presence of the  $2\Delta\mathbf{q}$  spin component was recently confirmed firmly by NMR (Ref. 30) and neutron-diffraction<sup>31</sup> experiments.

In  $\text{CuGeO}_3$ , a soft mode has not yet been found and it is now believed that there is no soft mode. On the other hand, there should be spin-phonon coupled mode(s) in  $\text{CuGeO}_3$ , because a spin-Peierls transition occurs in it. Therefore, finding a spin-phonon coupled mode is very important for understanding various phenomena in  $\text{CuGeO}_3$ . In this paper, studies of spin-phonon coupled modes near  $98\text{ cm}^{-1}$  are extended to doped  $\text{CuGeO}_3$ , and the behaviors of these modes will be clarified in the *D*, IC, DAF, and IAF phases.

## II. EXPERIMENT

Doped  $\text{CuGeO}_3$  single crystals were grown by a floating-zone method using an image furnace, and were cleaved along the (100) plane. A sample of  $\text{CuGe}_{0.988}\text{Si}_{0.012}\text{O}_3$  with dimensions of  $1.5\times 4\times 6\text{ mm}^3$  was used in this study. It showed two phase transitions, *U-D* and *D-DAF*, at low temperatures in zero field.

Far-infrared (FIR) transmission was measured in the spectral range between 15 and  $350\text{ cm}^{-1}$ , with a maximum resolution of  $0.1\text{ cm}^{-1}$  using a Fourier transform spectrometer (BOMEM DA8). The polarized measurements were performed in zero field by using FIR polarizers. The unpolarized magneto-optical spectra were obtained with a superconducting magnet in the Faraday configuration. The temperature dependence of the spectra was investigated down to 2 K. The spectra on the increasing (decreasing) field process were taken with a fixed field for several hours after increasing (decreasing) the applied magnetic field from a lower (higher) field region.

## III. RESULTS

The doping effect of the folded mode at  $98\text{ cm}^{-1}$  was investigated on  $\text{CuGe}_{0.988}\text{Si}_{0.012}\text{O}_3$  in the *D*, IC, DAF, and IAF phases. The transmission spectra were normalized by the spectrum in the *U* phase,  $\text{Tr}(T=17\text{ K}, B=0\text{ T})$ , in order to clarify the small change between the *U* phase and other phases. The inset of Fig. 1 shows the normalized transmission spectra,  $\text{Tr}(T)/\text{Tr}(T=17\text{ K})$ , at  $B=0\text{ T}$  on the doped sample. The spectra were taken when the sample was rotated around the *b* axis by  $30^\circ$ , so that the *a* axis was  $30^\circ$  from the incident light direction (see Fig. 3 of Ref. 25), because an absorption line at  $98\text{ cm}^{-1}$  was assigned to the  $B_{3M}$  folded-phonon mode with the polarization property of  $\mathbf{E}\parallel a$ .<sup>25</sup> The absorption appears at  $98\text{ cm}^{-1}$  below  $T_{SP}$ , and grows with decreasing temperature. Hereafter, the folded mode at  $98\text{ cm}^{-1}$  is labeled as FP. Figure 1 shows the absorption intensity of the FP mode of  $\text{CuGe}_{0.988}\text{Si}_{0.012}\text{O}_3$  as a function of temperature, together with that of the pure  $\text{CuGeO}_3$ . The solid lines show the best-fitted function  $(1-T/T_{SP})^{2\beta}$ , where the best-fitted value of  $2\beta$  for the doped  $\text{CuGeO}_3$  is

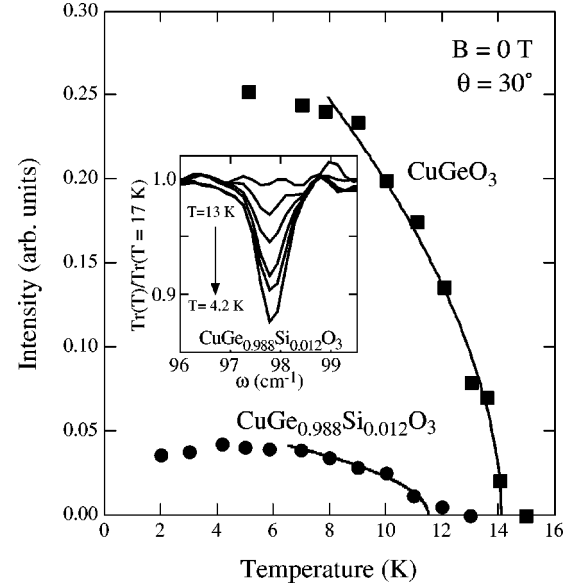


FIG. 1. Temperature dependence of the intensity of the FP mode on  $\text{CuGe}_{0.988}\text{Si}_{0.012}\text{O}_3$  and  $\text{CuGeO}_3$  in zero field with the samples rotated  $30^\circ$  around the *b* axis. The solid lines indicate the best-fitted functions of  $(1-T/T_{SP})^{2\beta}$ . The best-fitted values of  $2\beta$  are 0.55 and 0.5 for pure and doped  $\text{CuGeO}_3$ , respectively. The inset shows that the absorption of the FP mode increases with decreasing temperature down to  $T_N\approx 3.5\text{ K}$  on  $\text{CuGe}_{0.988}\text{Si}_{0.012}\text{O}_3$ .

0.5, and that for the pure  $\text{CuGeO}_3$  is 0.55.<sup>25</sup> The dependence on the temperature around  $T_{SP}$  is described well by the function  $(1-T/T_{SP})^{2\beta}$ , while the SP transition of the doped  $\text{CuGeO}_3$  seems to be somewhat less sharp and the FP mode was observed even just above  $T_{SP}$ , as observed on other folded modes on the Raman spectra.<sup>32</sup> The intensity of the superlattice reflections of the doped  $\text{CuGeO}_3$  exhibits a similar temperature dependence.<sup>10-12</sup>  $T_{SP}$  of the doped sample shifts toward a lower temperature.<sup>6</sup> The FP mode was also observed below  $T_N\approx 3.5\text{ K}$ , with the same peak energy and linewidth as in the *D* phase. The absorption intensity of the FP mode has a broad maximum around 4 K, and decreases slightly with temperature in the DAF phase.

Figure 2 shows the field dependence of the FP mode of the doped  $\text{CuGeO}_3$  at  $T=2\text{ K}$  on the decreasing field process, with the sample rotated around the *b* axis by about  $20^\circ$ . The region below  $H_C$  belongs to the DAF phase, and that above  $H_C$  belongs to the IAF phase. The splitting of the FP mode into two branches, which are labeled  $\text{FP}_U$  and  $\text{FP}_L$  in Fig. 2, were observed above  $H_C$  in doped  $\text{CuGeO}_3$ , as was observed in pure  $\text{CuGeO}_3$  at the transition from the *D* phase to the IC phase.<sup>25</sup> The energy separation  $\Delta\omega$  between  $\text{FP}_U$  and  $\text{FP}_L$  modes increases with the field.  $H_C$  of the doped  $\text{CuGeO}_3$  is lower than that of the pure one, as observed in Ref. 33. The coexistence of FP,  $\text{FP}_U$ , and  $\text{FP}_L$  modes was observed around  $H_C$  on the doped sample. The intensities of  $\text{FP}_U$  and  $\text{FP}_L$  modes in the higher-field region are almost equal to each other, and roughly a quarter of that of the FP mode in zero field. The halfwidths of  $\text{FP}_U$  and  $\text{FP}_L$  modes are almost the same as that of the FP mode, while it is dif-

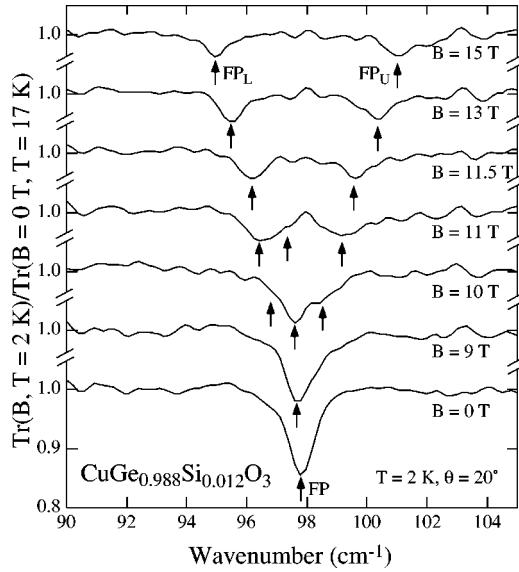


FIG. 2. Field dependence of the  $98 \text{ cm}^{-1}$  folded mode of  $\text{CuGe}_{0.988}\text{Si}_{0.012}\text{O}_3$  at 2 K, with the sample inclined around the  $b$  axis by about  $20^\circ$  from the Faraday configuration ( $\mathbf{B} \parallel \mathbf{a}$ ).

difficult to estimate them around  $H_C$ , owing to the overlap of the lines.

The peak energies of FP,  $\text{FP}_U$ , and  $\text{FP}_L$  modes on  $\text{CuGe}_{0.988}\text{Si}_{0.012}\text{O}_3$  are plotted in Fig. 3(a) as functions of the applied magnetic field on both the increasing and decreasing field processes. For reference, the field dependences of  $\text{CuGeO}_3$  are also plotted in Fig. 3(a). The energies of the FP modes do not depend on the applied field below  $H_C$ . A shift of the FP mode toward lower energies around  $H_C$  was observed on the doped sample, but the amount of the shift is much smaller than that of the pure sample. The positions of  $\text{FP}_U$  and  $\text{FP}_L$  modes are symmetrical with respect to that of the FP mode of  $H \leq H_C$  on both pure and doped  $\text{CuGeO}_3$ .  $\Delta\omega$  increased with the field above  $H_C$ , and the rate of change of  $\Delta\omega$  with respect to the applied field decreases gradually with increasing field. The difference of behaviors between pure and doped  $\text{CuGeO}_3$  was observed on the field dependence of  $\Delta\omega$  around  $H_C$ ; that is, the increasing rate of  $\Delta\omega$  on the doped  $\text{CuGeO}_3$  is relatively lower than that on the pure one. The field dependence of FP,  $\text{FP}_U$ , and  $\text{FP}_L$  modes on  $\text{CuGeO}_3$  exhibits a hysteresis around  $H_C$ . The presence of the hysteresis means that the transition between the  $D$  and IC phases is of first order even in the doped sample, and this corresponds to the fact that the hysteresis is also observed in pure  $\text{CuGeO}_3$  in magnetization,<sup>6</sup> magnetostriction<sup>34</sup> and the incommensurability of the lattice modulation.<sup>7</sup> The amounts of the hysteresis of  $\text{FP}_U$  and  $\text{FP}_L$  modes on both the pure and doped samples are about  $\Delta B_H \approx 0.2 \text{ T}$  in the region of  $\Delta\omega \approx 3 \text{ cm}^{-1}$ , which were estimated by difference between the magnetic fields, where  $\Delta\omega$ 's are equal to each other in increasing and decreasing field processes. They are almost independent of the field around  $H_C$ . In the doped sample, the remnant signal of the FP mode on the increasing field process and those of  $\text{FP}_U$  and  $\text{FP}_L$  modes on the decreasing field process were observed in a relatively wide range of  $\Delta B_R \approx 0.4 \text{ T}$ . The remnant signals have not been observed in the

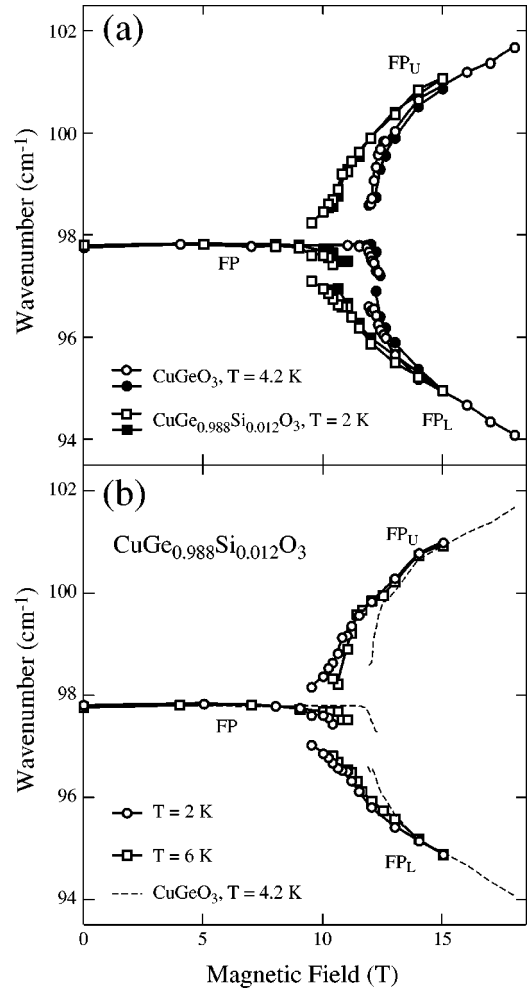


FIG. 3. (a) Field dependence of the peak positions of FP,  $\text{FP}_U$ , and  $\text{FP}_L$  modes at  $T = 2 \text{ K}$  on  $\text{CuGe}_{0.988}\text{Si}_{0.012}\text{O}_3$ , and at  $T = 4.2 \text{ K}$  on  $\text{CuGeO}_3$  (Ref. 45), when the sample is rotated by  $20^\circ$  from the Faraday configuration ( $\mathbf{B} \parallel \mathbf{a}$ ). Open symbols show the data for the decreasing field process, and closed symbols that for the increasing field process. Hysteresis appears around the critical field  $H_C$ . (b) Field dependence of the energy positions of FP,  $\text{FP}_U$ , and  $\text{FP}_L$  modes at  $T = 2$  and  $6 \text{ K}$  on  $\text{CuGe}_{0.988}\text{Si}_{0.012}\text{O}_3$  on the decreasing field process. The broken lines show the field dependences of these peak energies on  $\text{CuGeO}_3$  at  $T = 4.2 \text{ K}$ , for reference.

pure  $\text{CuGeO}_3$ . The slow field dependence and the remnant signals of these branches make the coexistence region of the doped  $\text{CuGeO}_3$  much wider than that of the pure one. An enhancement of the coexistence region on the doped  $\text{CuGeO}_3$  was also observed by x-ray experiments.<sup>35</sup> Hereafter, we show only the field dependence of FP,  $\text{FP}_U$ , and  $\text{FP}_L$  modes on the decreasing field process.

Figure 3(b) shows the field dependences of the peak energies of FP,  $\text{FP}_U$ , and  $\text{FP}_L$  modes on  $\text{CuGe}_{0.988}\text{Si}_{0.012}\text{O}_3$  at  $T = 6 \text{ K}$  together with those at  $T = 2 \text{ K}$ . The broken lines show the field dependences of these peak energies on  $\text{CuGeO}_3$  at  $T = 4.2 \text{ K}$ , for reference. The region near  $6 \text{ K}$  is well above  $T_N$  at  $B = 0 \text{ T}$ , and therefore at  $B \sim 15 \text{ T}$  it should belong to the  $U$  phase according to Ref. 16 or to the IC phase according to Refs. 15 and 17. This shows, defi-

nately, that the FP mode is split into two modes  $FP_U$  and  $FP_L$  above  $H_C \sim 10.5$  T. This fact clearly shows that a phase with an incommensurate structure exists above  $H_C$  at  $T=6$  K, which we may call the IC phase. Therefore, we have confirmed that the phase diagram obtained in Refs. 15 and 17 is realized in  $\text{CuGe}_{0.988}\text{Si}_{0.012}\text{O}_3$ . The field dependence of  $FP_U$  and  $FP_L$  modes at  $T=6$  K is slightly steeper than that at  $T=2$  K in the region of  $\Delta\omega < 3$   $\text{cm}^{-1}$ . On the other hand, it overlaps with that at  $T=2$  K in the region of  $\Delta\omega > 3$   $\text{cm}^{-1}$ . The remnant signals were also observed at  $T=6$  K, but the field range is much narrower than that at  $T=2$  K.

#### IV. DISCUSSION

In this study, the doping effect of the folded mode FP was investigated in the  $D$ , IC, DAF, and IAF phases on doped  $\text{CuGeO}_3$ . The folded mode FP appears on the doped sample below  $T_{SP}$ , and the peak energy is independent of the doping in the  $D$  phase. The intensity of the doped sample is much weaker than that of the pure one. A similar behavior was seen in the absorption intensity of the  $800\text{-cm}^{-1}$  folded-phonon mode.<sup>36</sup> The halfwidth of the FP mode on the  $\text{CuGe}_{0.988}\text{Si}_{0.012}\text{O}_3$  is about 1.5 times wider than that on the pure  $\text{CuGeO}_3$ . There are few reports on the effects of doping on the halfwidth of other folded-phonon modes. The effect on the Raman-active  $369\text{-cm}^{-1}$  mode is unclear due to the low resolution of the measuring system.<sup>37</sup> The effect on the halfwidth of the infrared-active  $800\text{-cm}^{-1}$  mode is not estimated, although the halfwidth seems to be somewhat broadened in Fig. 10 of Ref. 36.

The FP mode was observed below  $T_N$ , because of the presence of the lattice modulation of  $\mathbf{q}_{SP}$ .<sup>10–12</sup> Figure 1 shows that the intensity of the doped sample decreases below  $T_N \approx 3.5$  K with temperature. This means that the dimerization is suppressed with the growth of the antiferromagnetic long-range order. This indicates that the dimerization (the SP order parameter) coexists with the antiferromagnetic long-range order in the DAF phase, and that these two order parameters interact with each other. In neutron-diffraction measurements, the superlattice reflection peak was found to coexist with the antiferromagnetic peak and the intensity of the superlattice reflection decreases.<sup>10–12</sup> The temperature dependence of the intensity of the FP mode is fully consistent with that of the superlattice reflection, because the intensity of the folded phonons is closely related to the magnitude of the lattice distortion caused by the dimerization due to the SP ordering.

Above  $H_C$ , the splitting into  $FP_U$  and  $FP_L$  modes was observed in the IC and IAF phases on the doped sample. Based on our model<sup>25</sup> of the splitting of the folded-phonon FP, the necessary conditions for splitting are not only the spin-phonon coupling but also the existence of the lattice modulation of  $\pm(\mathbf{q}_{SP} - \Delta\mathbf{q})$  and the component of the spin polarization with the periodicity of  $2\Delta\mathbf{q}$ . Therefore, experimental results indicate the existence of an incommensurate modulation in the lattice and a spin polarization in both the IC and IAF phases. The incommensurate lattice modulation was observed in the IC and IAF phases on doped samples in

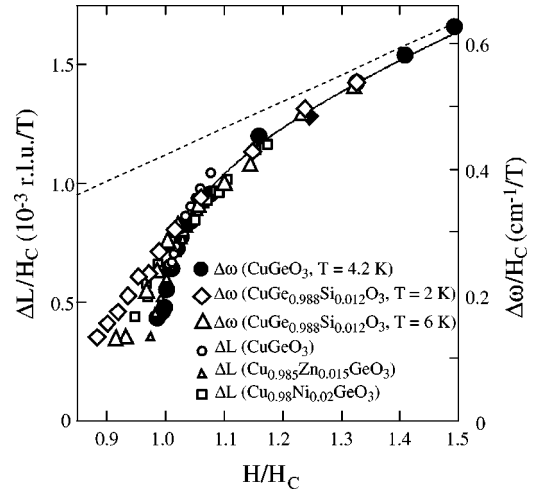


FIG. 4. Scaled field dependence of the energy separation  $\Delta\omega$  between the two split branches at  $T=2$  and  $6$  K on  $\text{CuGe}_{0.988}\text{Si}_{0.012}\text{O}_3$ , and at  $T=4.2$  K on  $\text{CuGeO}_3$  (Ref. 45). The same for the superlattice reflections,  $\Delta L$ , on both the pure and doped  $\text{CuGeO}_3$  are also plotted simultaneously, where  $\Delta L$  was measured by Kiryukhin *et al.* (Ref. 8). Both  $\Delta\omega$  and  $\Delta L$  were scaled by the respective critical field  $H_C$ . The dashed line indicates the theoretical prediction by Cross for the high magnetic field limit (Ref. 39). The solid curve is the fitting function  $1/\ln[8/(H/H_C - 1)]$ , which was predicted by mean-field theory (Ref. 38).

x-ray-diffraction experiments.<sup>35</sup> A behavior of the splitting different from that for pure  $\text{CuGeO}_3$  was found around  $H_C$ . That is, the field dependence of the peak positions of the  $FP_U$  and  $FP_L$  modes on the doped  $\text{CuGeO}_3$  are relatively slower than that on the pure one. Moreover, the field dependence at  $T=2$  K is slightly weaker than that at  $T=6$  K in the vicinity of  $H_C$ , while the field dependences at  $T=2$  K, and  $6$  K almost overlap with each other in the higher field region. The positions of  $FP_U$  and  $FP_L$  modes in the IC and IAF phases of the doped sample gradually approach those of the pure sample with increasing field, which means that their field dependences can be well described by the same function at a higher field range.

In our previous paper, it was shown that the field dependence of  $\Delta\omega$  can be scaled with that of the incommensurability,  $\Delta L$ , and we concluded that  $\Delta\omega$  is proportional to  $\Delta L$  in pure  $\text{CuGeO}_3$ .<sup>25</sup> In order to clarify the difference between pure and doped  $\text{CuGeO}_3$ ,  $\Delta\omega$ 's of doped  $\text{CuGeO}_3$  in the IAF and IC phases are plotted by scaling them with  $H_C$ , as well as  $\Delta\omega$  of the pure  $\text{CuGeO}_3$  and  $\Delta L$  in the x-ray experiments, as shown in Fig. 4. The critical fields  $H_C$  of the doped  $\text{CuGeO}_3$  are determined to fit the field dependence of  $\Delta\omega$  in the fitting function, especially in the higher field range where the similarity to the pure  $\text{CuGeO}_3$  was observed, because it is difficult to define the correct  $H_C$  of the doped  $\text{CuGeO}_3$  owing to the wide coexistent region. The scale of the right-side ordinate for  $\Delta\omega$  is the same as that of the pure  $\text{CuGeO}_3$ , which is adjusted to fit the field dependence of  $\Delta\omega$  to that of  $\Delta L$ . The solid curve in Fig. 4 is the fitting function  $1/\ln[8/(H/H_C - 1)]$ .<sup>38</sup> The dashed line indicates the theoretical prediction of Cross for the high-magnetic-field limit.<sup>39</sup> Figure 4 indicates that  $\Delta\omega$  of the doped  $\text{CuGeO}_3$  deviates

from the fitting function in the IAF and IC phases in the lower field range of  $H/H_C < 1.03$ , and is observed even at  $H/H_C < 1$ , while it can be plotted quite well on the same universal curve as that of the pure sample at the higher field region of  $H/H_C > 1.03$ . The discrepancy increases with decreasing  $\Delta\omega$  around  $H_C$ . A similar behavior can be seen on  $\Delta L$  of the doped  $\text{CuGeO}_3$  sample, especially, with a higher concentration of impurities,<sup>8</sup> as shown in Fig. 4. In the IAF phase, the discrepancy is larger than that in the IC phase on the doped  $\text{CuGeO}_3$ , and  $\Delta\omega$  in the IAF phases survives at the lower field on the  $H/H_C$  scale. This result indicates that  $\Delta\omega$  and  $\Delta L$  are no longer described by the fitting function at this field range. This does not necessarily mean that the relation  $\Delta\omega \propto \Delta L$  is broken in this region, because  $\Delta\omega$  and  $\Delta L$  were measured on different samples. In the higher field region of  $H/H_C > 1.03$ ,  $\Delta L$  is well described by the same theoretical fitting function on both pure and doped  $\text{CuGeO}_3$ . Therefore, the proportional relation of  $\Delta\omega \propto \Delta L$  may be valid even on the doped  $\text{CuGeO}_3$  at  $H/H_C > 1.03$ . We assumed that the strength of the coupling is proportional to the density of the solitons with periodicity  $2\Delta\mathbf{q}$ , i.e., the integrated intensity of the average component of the spin polarization of  $2\Delta\mathbf{q}$ .<sup>25</sup> Consequently,  $\Delta\omega$  is determined only by the incommensurability,  $\Delta L$ , and is independent of the species of the impurities or the mechanism of how the local magnetization is induced around the impurities.<sup>40,41</sup>  $\Delta\omega$  gradually approaches the curve predicted by the theory of Cross with increasing field, and seems to approach the theory of Cross above  $H/H_C \approx 1.5$ . In the field range of  $H/H_C \geq 1.5$ , the field dependence of the magnetization<sup>6,30</sup> and the spontaneous strain<sup>42,43</sup> can be fitted by a linear function, and the lattice modulation is well described as sinusoidal.<sup>42</sup> The discrepancy between the pure and doped  $\text{CuGeO}_3$  around  $H_C$  can be explained by the presence of an interaction between the solitons and the impurities, as follows. The interaction between the solitons and impurities must exist on the doped  $\text{CuGeO}_3$ , and a binding of the solitons to the impurities can occur.<sup>41,44</sup>

They change the distribution of intersoliton distance, and induces randomness in it. The effect of the interaction is enhanced on the condition that the number of solitons is of the same order as that of the impurities, and is weakened with increasing soliton numbers as compared with the impurity numbers. Therefore, in the higher field region, the effect of this interaction is weak, and  $\Delta\omega$  and  $\Delta L$  exhibit almost the same field dependence as that of the pure  $\text{CuGeO}_3$ . On the other hand, around  $H_C$ , the effect of the interaction is no longer negligible, and the randomness prevents  $H_C$  from being well defined, which makes the field dependence of  $\Delta\omega$  weaker. The different behavior of  $\Delta\omega$  between the IAF and IC phases indicates that the impurity effect in the IAF phase is stronger than that in the IC phase. This is consistent with the model of ‘‘freezing’’ of the solitons in the IAF phase.<sup>17</sup> The observation of remnant signals in the IAF phase could also be related to the freezing of the solitons. Interestingly, the interaction between the solitons and the impurities, or the freezing of the solitons, does not affect the hysteresis of the  $\text{FP}_L$  and  $\text{FP}_U$  modes. The reduction of the shift of the FP mode in the vicinity of  $H_C$  might be connected with this interaction if, as we believe, the shift of the FP mode is caused by the discommensuration which appears just above  $H_C$ .

## V. CONCLUSIONS

We have performed the doping effect for a folded-phonon mode at  $98 \text{ cm}^{-1}$  on Si-doped  $\text{CuGeO}_3$ . The folded-phonon mode was observed in both the  $D$  and DAF phases, and the splitting of the mode was observed in IC and IAF phases. This definitely proves that the IC phase exists in the regions of  $T_N \leq T \leq T_{SP}$  and  $H \geq H_C$ , which is consistent with the reports of Refs. 15 and 17. The different behavior of the split-off branches from the pure  $\text{CuGeO}_3$  was observed in the vicinity of  $H_C$ , and the discrepancy in the IAF phase is larger than that in the IC phase. This is explained by the interaction between the solitons and impurities.

<sup>1</sup>M. Hase, I. Terasaki, and K. Uchinokura, Phys. Rev. Lett. **70**, 3651 (1993).

<sup>2</sup>O. Kamimura, M. Terauchi, M. Tanaka, O. Fujita, and J. Akimitsu, J. Phys. Soc. Jpn. **63**, 2467 (1994).

<sup>3</sup>J.P. Pouget, L.P. Regnault, M. Ain, B. Hennion, J.P. Renard, P. Veillet, G. Dhalenne, and A. Revcolevschi, Phys. Rev. Lett. **72**, 4037 (1994).

<sup>4</sup>K. Hirota, D.E. Cox, J.E. Lorenzo, G. Shirane, J.M. Tranquada, M. Hase, K. Uchinokura, H. Kojima, Y. Shibuya, and I. Tanaka, Phys. Rev. Lett. **73**, 736 (1994).

<sup>5</sup>M. Nishi, O. Fujita, and J. Akimitsu, Phys. Rev. B **50**, 6508 (1994).

<sup>6</sup>M. Hase, I. Terasaki, K. Uchinokura, M. Tokunaga, N. Miura, and H. Obara, Phys. Rev. B **48**, 9616 (1993).

<sup>7</sup>V. Kiryukhin and B. Keimer, Phys. Rev. B **52**, R704 (1995).

<sup>8</sup>V. Kiryukhin, B. Keimer, J.P. Hill, and A. Vigliante, Phys. Rev. Lett. **76**, 4608 (1996).

<sup>9</sup>M. Hase, I. Terasaki, Y. Sasago, K. Uchinokura, and H. Obara,

Phys. Rev. Lett. **71**, 4059 (1993).

<sup>10</sup>L.P. Regnault, J.P. Renard, G. Dhalenne, and A. Revcolevschi, Europhys. Lett. **32**, 579 (1995).

<sup>11</sup>Y. Sasago, N. Koide, K. Uchinokura, M.C. Martin, M. Hase, K. Hirota, and G. Shirane, Phys. Rev. B **54**, R6835 (1996).

<sup>12</sup>M.C. Martin, M. Hase, K. Hirota, G. Shirane, Y. Sasago, N. Koide, and K. Uchinokura, Phys. Rev. B **56**, 3173 (1997).

<sup>13</sup>T. Masuda, A. Fujioka, Y. Uchiyama, I. Tsukada, and K. Uchinokura, Phys. Rev. Lett. **80**, 4566 (1998).

<sup>14</sup>T. Masuda and K. Uchinokura, Physica B **284-288**, 1637 (2000).

<sup>15</sup>M. Hiroi, T. Hamamoto, M. Sera, H. Mojiri, N. Kobayashi, M. Motokawa, O. Fujita, A. Ogiwara, and J. Akimitsu, Phys. Rev. B **55**, R6125 (1996).

<sup>16</sup>M. Poirier, R. Beaudry, M. Castonguay, M.L. Plumer, G. Quirion, F.S. Razavi, A. Revcolevschi, and G. Dhalenne, Phys. Rev. B **52**, R6971 (1995).

<sup>17</sup>J. Takeya, I. Tsukada, Y. Ando, T. Masuda, K. Uchinokura, I.

- Tanaka, R.S. Feigelson, and A. Kapitulnik, *Phys. Rev. B* **63**, 214407 (2001).
- <sup>18</sup>H. Völlenkle, A. Wittmann, and H. Nowotny, *Monatsch. Chem.* **98**, 1352 (1967).
- <sup>19</sup>M. Braden, G. Wilkendorf, J. Lorenzana, M. Aïn, G.J. McIntyre, M. Behruzi, G. Heger, G. Dhalenne, and A. Revcolevschi, *Phys. Rev. B* **54**, 1105 (1996).
- <sup>20</sup>H. Kuroe, T. Sekine, M. Hase, Y. Sasago, K. Uchinokura, H. Kojima, I. Tanaka, and Y. Shibuya, *Phys. Rev. B* **50**, 16 468 (1994).
- <sup>21</sup>N. Ogita, T. Minami, Y. Tanimoto, O. Fujita, J. Akimitsu, P. Lemmens, G. Güntherodt, and M. Udagawa, *J. Phys. Soc. Jpn.* **65**, 3754 (1996).
- <sup>22</sup>P.H.M. van Loosdrecht, J.P. Boucher, G. Martinez, G. Dhalenne, and A. Revcolevschi, *Phys. Rev. Lett.* **76**, 311 (1996).
- <sup>23</sup>A. Damascelli, D. van der Marel, F. Parmigiani, G. Dhalenne, and A. Revcolevschi, *Phys. Rev. B* **56**, R11 373 (1997).
- <sup>24</sup>M.N. Popova, A.B. Sushkov, S.A. Golubchik, A.N. Vasil'ev, and L.I. Leonyuk, *Phys. Rev. B* **57**, 5040 (1998).
- <sup>25</sup>K. Takehana, T. Takamasu, M. Hase, G. Kido, and K. Uchinokura, *Phys. Rev. B* **62**, 5191 (2000).
- <sup>26</sup>P.H.M. van Loosdrecht, J.P. Boucher, G. Martinez, G. Dhalenne, and A. Revcolevschi, *J. Appl. Phys.* **79**, 5395 (1996).
- <sup>27</sup>I. Loa, S. Gronemeyer, C. Thomsen, and R.K. Kremer, *Z. Phys. Chem. (Munich)* **201**, 333 (1997).
- <sup>28</sup>J.L. Musfeldt, Y.J. Wang, S. Jandl, M. Poirier, A. Revcolevschi, and G. Dhalenne, *Phys. Rev. B* **54**, 469 (1996).
- <sup>29</sup>T. Janssen, *J. Phys. C* **12**, 5391 (1979).
- <sup>30</sup>M. Horvatić, Y. Fagot-Revurat, C. Berthier, G. Dhalenne, and A. Revcolevschi, *Phys. Rev. Lett.* **83**, 420 (1999).
- <sup>31</sup>H.M. Rønnow, M. Enderle, D.F. McMorrow, L.-P. Regnault, G. Dhalenne, A. Revcolevschi, A. Hoser, K. Prokes, P. Vorderwisch, and H. Schneider, *Phys. Rev. Lett.* **84**, 4469 (2000).
- <sup>32</sup>H. Kuroe, J. Sasaki, T. Sekine, T. Masuda, N. Koide, I. Tsukada, and K. Uchinokura, *J. Phys. Soc. Jpn.* **68**, 2046 (1999).
- <sup>33</sup>M. Hase, Y. Sasago, I. Terasaki, K. Uchinokura, G. Kido, and T. Hamamoto, *J. Phys. Soc. Jpn.* **65**, 272 (1996).
- <sup>34</sup>K. Takehana, M. Oshikiri, G. Kido, M. Hase, and K. Uchinokura, *J. Phys. Soc. Jpn.* **65**, 2783 (1996).
- <sup>35</sup>V. Kiryukhin, B. Keimer, J.P. Hill, S.M. Coad, and D.McK. Paul, *Phys. Rev. B* **54**, 7269 (2000).
- <sup>36</sup>A. Damascelli, D. van der Marel, G. Dhalenne, and A. Revcolevschi, *Phys. Rev. B* **61**, 12 063 (2000).
- <sup>37</sup>H. Kuroe, J. Sasaki, T. Sekine, Y. Sasago, M. Hase, N. Koide, K. Uchinokura, H. Kojima, I. Tanaka, and Y. Shibuya, *Physica B* **219-220**, 104 (1996).
- <sup>38</sup>A.I. Buzdin, M.L. Kubic, and V.V. Tugushev, *Solid State Commun.* **48**, 483 (1983).
- <sup>39</sup>M.C. Cross, *Phys. Rev. B* **20**, 4606 (1979).
- <sup>40</sup>H. Fukuyama, T. Tanimoto, and M. Saito, *J. Phys. Soc. Jpn.* **65**, 1182 (1996).
- <sup>41</sup>P. Hansen, D. Augier, J. Riera, and D. Poilblanc, *Phys. Rev. B* **59**, 13 557 (1999).
- <sup>42</sup>T. Lorenz, B. Bücher, P.H.M. van Loosdrecht, F. Schönfeld, G. Chouteau, A. Revcolevschi, and G. Dhalenne, *Phys. Rev. Lett.* **81**, 148 (1998).
- <sup>43</sup>K. Takehana, T. Takamasu, M. Hase, G. Kido, and K. Uchinokura, *Physica B* **246-247**, 246 (1998).
- <sup>44</sup>D. Augier, P. Hansen, D. Poilblanc, J. Riera, and E. Sørensen, *cond-mat/9807265* (unpublished).
- <sup>45</sup> $\Delta\omega$  of the pure  $\text{CuGeO}_3$  in Fig. 4 was reexamined in this study, because the hysteresis was not taken into account in Ref. 25.